

## Invited

## InAs-GaAs Quantum Dot Lasers: in Situ Growth, Radiative Lifetimes and Polarization Properties

D. Bimberg, N.N. Ledentsov\*, N. Kirstaedter, O. Schmidt, M. Grundmann

*Institut für Festkörperphysik, TU Berlin, Hardenbergstr. 36, D-10623 Berlin, Germany*

V.M. Ustinov, A.Yu. Egorov, A.E. Zhukov, M.V. Maximov, P.S. Kop'ev and Zh.I. Alferov

*A.F.Ioffe Physical-Technical Institute, Politehnicheskaya 26, 194021, St.Petersburg, Russia*

S.S. Ruvimov\*, U. Gösele and J. Heydenreich

*Max-Planck-Institut für Mikrostrukturphysik, Weinberg 2, D-06120 Halle, Germany*

InAs-GaAs and InGaAs-GaAs diode laser structures with small  $\sim 60\text{-}80\text{\AA}$  quantum dots (QDs) exhibit *low threshold current densities* (below  $100\text{ A}\cdot\text{cm}^{-2}$ ) and *ultrahigh* characteristic temperatures ( $T_0=350\text{-}425\text{K}$ ) for  $T < 100 - 150\text{K}$ . For higher temperatures  $T_0$  decreases and the threshold current density increases mainly due to carrier evaporation from the QDs. Larger dots provide better carrier localization but exhibit saturation of the QD emission, enhanced nonradiative recombination rate at high excitation densities and longer radiative lifetimes.

### 1 INTRODUCTION

Quantum dot diode lasers are expected to have superior properties with as compared to quantum well (QW lasers). High differential gain, ultralow threshold current density and high temperature stability of threshold current density are expected to occur simultaneously [1, 2].

After a critical amount of strained material is deposited on the substrate formation of coherent strained islands on the bare substrate for Volmer-Weber (VW) growth or on the wetted surface for coherent Stranski-Krastanow (SK) growth occurs. Experiments show in most cases rather narrow size distribution of the 3D islands [3, 4, 5]. This is not an effect due to SK or VW growth modes themselves. We have considered several realistic shapes of strained islands [6]. First we establish that islands with well defined side facets and *no* planar top surface are energetically more favourable than islands with a flat top surface. Second we have compared the total energies of different arrays of strained islands interacting via the strained substrate. A periodic array of pyramid-like coherent islands of the same identical size arranged in a 2D square lattice with main axes along the [001] and [010] directions corresponds, under certain conditions, to a minimum of total energy [6].

### 2. EXPERIMENTAL

All samples were grown by elemental source molecular beam epitaxy (MBE) on GaAs (100) substrates using RIBER-32 and EP1203 MBE machines. The lasers were fabricated in a shallow stripe ( $W=25\text{ }\mu\text{m}$ ) geometry. Details of the growth and processing are published elsewhere [7]. Transmission electron microscopy (TEM) studies were performed using a high voltage JEOL JEM1000 (1MV) microscope. For PL studies of the laser structures the top GaAs contact layer was etched off. Undoped structures grown in the identical geometry as the laser structures were used for lifetime and excitation density studies to exclude the p-n junction-induced effects.

Dots formed after the critical layer thickness is just exceeded ( $5\text{-}6\text{\AA}$  InAs) are small, mostly do not show well resolved crystalline shape, and exhibit large size dispersion. Increase in the amount of InAs deposited to 4 ML results in a dense array of well-developed dots having a size of  $\sim 140\text{ }\text{\AA}$  and a height of  $\sim 60\text{ }\text{\AA}$ . The sides of the square-shaped base of the dots are parallel to either [001] or [010] directions. The smaller size of the dots in the case of the 2 ML sample ( $70\text{-}80\text{\AA}$ ) agrees well with a strong shift of the corresponding PL line towards higher photon energies. We have found that the introduction of growth interruption of 40 s (10 s) after InAs is deposited is enough to let the dot to reach the equilibrium size for 2.5 ML (3 ML) InAs deposition [8].

### 3 ENERGY SPECTRUM

Detailed theoretical calculations of strain distribution and electronic structure of pyramid-like InAs quantum dots having a size of  $\sim 140\text{ }\text{\AA}$  with {101}-like side facets including piezoelectric and excitonic effects have been carried out in [9] with the result that only one electron but several hole states exist. Only  $|3/2, 3/2\rangle$  hole states play a role. Under highly spatially resolved excitation with a focused electron beam, the luminescence spectrum consists of a series of ultranarrow ( $< 0.15\text{ meV}$ ) lines, each originating from a single InAs quantum dot [10]. The *lines do not exhibit broadening with temperature increase*, directly indicating the atomic-like electronic spectrum of a single dot [10].

### 4 InAs-GaAs QUANTUM DOT LASERS

The exciton ground state wavefunction is effectively localized in the InAs QDs. Even in the case of a very dense array of quantum dots (4 ML InAs) only  $\sim 2\text{ ML}$  InAs is transferred into dots. The effective exciton volume averaged over the surface area is below  $6\text{\AA}$  resulting in an extremely small optical confinement factor.

Fig. 1 a presents results of luminescence lifetime and excitation density dependence studies of QDs formed by  $5\text{ }\text{\AA}$  InAs deposition. Electroluminescence (EL) and PL spectra are depicted in Fig. 1 b and c, respectively. Both QD ( $\sim 1.26\text{ eV}$ ) and wetting layer (WL) PL ( $1.42\text{ eV}$ ) peaks are clearly resolved in Fig. 1 c. The dot growth is kinetically-controlled in this case and the size dispersion is relatively large giving a possibility to monitor the lifetime and the electroluminescence as function of dots size within the *same* sample. Another advantage of the sample is the larger dot density (around  $6 \times 10^{10}\text{ cm}^{-2}$ )

$7 \cdot 10^{10} \text{ cm}^{-2}$ ) as compared to equilibrium dots (typically  $3\text{-}4 \cdot 10^{10} \text{ cm}^{-2}$  at  $T_s=480^\circ\text{C}$ , respectively). The *average* dot size estimated from the PL peak maximum energy corresponds to dots having a  $\sim 70\text{-}80 \text{ \AA}$  base length. The energy separation between the electron QD energy level and the wetting layer energy level is relatively small in this case (around 20 - 60 meV). The dependence of the QD PL peak intensity on the excitation density is close to linear with a tendency towards saturation at highest excitation densities. The ground state QD radiative lifetime does not change with the excitation density being always close to 1.8 ns (1.2 - 1.3 eV), while the *spectrally averaged total* lifetime *decreases*. This is due to the increasing contribution of radiative recombination channels via smaller dots, wetting layer and GaAs states with the relative radiative recombination efficiency increasing with the excitation density rise. It is important to note that for larger *equilibrium* ( $t_{av}=4\text{ML InAs}$ ) dots the PL intensity saturates at much lower excitation densities partly due to the lower aerial density of these dots and slightly longer (2 ns) radiative lifetimes in this case. Despite quantum dots exhibit superior PL properties at low excitation densities as compared to quantum well structures both at low and at room temperatures, at high excitation densities not only the equilibrium quantum dot emission intensity saturates, but also the *integrated* PL intensity saturates indicating efficient nonradiative recombination channels which appear at high excitation densities. These results indicate intrinsic concentration-sensitive nonradiative recombination mechanisms, such as e.g. Auger recombination via the QD heavy hole excited states which may not be present in the case of the smaller dots (see Fig. 2).

A characteristic feature of the quantum dot edge EL emission is its partial depolarization as compared to the strained InGaAs quantum well case where the heavy-hole emission is 100% TE polarized. On the other hand the QD edge emission remains *predominantly* TE polarized. This fact reflects the symmetry of the heavy hole wavefunction in the quantum dot which is much more strongly squeezed in  $z$ -direction than in the  $x, y$  directions. At the same time, confinement in  $x, y$  directions results in partial *depolarization* of the quantum dot edge luminescence. For smaller dots having the *same* shape, the hole wavefunction becomes more symmetric. Thus the degree of polarization is further reduced at the high energy side of the EL spectra. The QD-related peaks revealed in PL and edge EL spectra coincide in energy. Wetting layer luminescence is also observed in both PL and EL spectra recorded from the top of the structure through a window in the contact layer. WL luminescence is not observed in the edge EL spectra due to its efficient self-absorption in the waveguide geometry.

For resonator cavity lengths around 1-1.5 mm the lasing at 77K starts at energies close to the QD PL maximum intensity energy *unambiguously* indicating that the *ground state* quantum dot transitions are responsible for lasing. For smaller resonator lengths the lasing energy continuously shifts to higher energies indicating that the *largest gain* is realized for the *smallest* dots. This result agrees fairly well with the results of spatially and time-resolved cathodoluminescence studies also indicating much smaller radiative lifetimes ( $\sim 0.2 - 0.3 \text{ ns}$ ) for smaller quantum dots (PL at 1.35 eV) [10] having a smaller localization energy (Rashba effect [11]).

In Fig. 2 we depict the dependence of the QD PL decay time, the QD and the WL PL energies, the lasing energy, the integrated PL intensity and the threshold current density on the temperature of observation for  $5\text{ \AA}$  InAs dots. The QD PL decay times being close to 1.5 ns, show the weak temperature dependence up to 100K. Moderate *increase* in the decay time most probably indicates the electron hopping between neighbouring quantum dots via the wetting layer. The energy separation between the electron levels in the wetting layer and in the  $70\text{-}75 \text{ \AA}$  InAs dot is around 20 meV and at finite temperatures the electron has a possibility to make several jumps between the different dots before radiative recombination occurs. The QD hole localization energy ( $\sim 90 \text{ meV}$ ) is too high to let the hole be evaporated to the wetting layer at temperatures below 100K and there is practically no change in the integrated PL intensity in this temperature range. The lasing energy is very close to the QD PL and EL maximum energies at low and at moderate excitation densities and the threshold current density remains effectively unaffected by the temperature increase. To the best of our knowledge, the characteristic temperature measured in this temperature range ( $T_0=425\text{K}$ ) is the highest reported up to now for semiconductor diode lasers. For further increase of the temperature above 100 K the integrated PL intensity start to decrease and the decay time of the QD PL and the QD PL intensity significantly shortens indicating the onset of efficient nonradiative recombination. The activation energy for this process measured from the logarithm of the QD PL intensity vs. reverse temperature dependence corresponds to 80-90 meV and points to efficient *hole* evaporation from the quantum dots to the wetting layer. The threshold current density shows an increase in the same temperature range and the lasing energy shifts towards the higher energy side of the QD emission corresponding to smaller dots having larger oscillator strength.

The effects observed in the higher temperature range above 100K are related to the insufficient gain realized in the laser structure. To increase the gain one needs either to reduce the width of the PL line while maintaining the dot size and shape, or to increase the dot density. Small (*kinetically controlled*) dots may be more easily stacked. Moreover, size uniformity is greatly improved in this case. Results on stacked dots arrays will be reported elsewhere [12].

QD lasers have been also realized using InGaAs quantum dots formed by submonolayer InAs and GaAs deposition [5, 7] at  $450^\circ\text{C}$  resulting in a very dense ( $\sim 3 \cdot 10^{11} \text{ cm}^{-2}$ ) array of small ( $\sim 60 \text{ \AA}$ ) uniform dots. The general trends in the device characteristics of the InGaAs QD laser [7] are similar to those for InAs QD laser.  $T_0$  is equal to 350K in the temperature range 50-150K and the threshold current density is about  $120 \text{ A.cm}^{-2}$ . InGaAs quantum dot electroluminescence is significantly depolarized like in the case of InAs QDs. Relatively small energy separation between the QD ground exciton state and the wetting layer states ( $\sim 100 \text{ meV}$ ) results in efficient evaporation of the excitons and carriers from the QDs at higher temperatures ( $>170\text{K}$ ). To compensate the resulting gain loss, the threshold current density is increased to  $950 \text{ A.cm}^{-2}$  at 300K.

Single longitudinal mode lasing is observed both at low and at high (300K) temperatures [7] in InGaAs QD lasers. The reason for the latter effect is not yet clear, but may be related to the quasiperiodic arrangement of InGaAs quantum dots and their agglomerations resulting in effective distributed feedback structure [5, 13].

## 5. CONCLUSION

The first QD laser structures have shown already several important advantages (low threshold current density, large  $T_0$  at  $T < 100\text{-}150\text{K}$ ). At the same time more efforts are required to overcome the remaining difficulties. This underlines the importance of both fundamental and applied research for better understanding the QD growth mechanism, their electronic spectra, carrier relaxation and recombination properties.

Acknowledgements: Various parts of this work are supported by Volkswagen-Stiftung, by INTAS-94-1028 grant and by Deutsche Forschungsgemeinschaft in the framework of Sfb 296. N.N.L. is grateful to Alexander von Humboldt Foundation.

\* on leave from A.F. Ioffe Physical Technical Institute

- 1 Y.Arakawa, H.Sakaki, *Appl.Phys.Lett*, **40**, pp. 939 (1982)
- 2 Y.Arakawa, A.Yariv, *IEEE J.Quantum.Electron.*, **QE22**, 1887 (1986)
- 3 D.Leonard, M.Krishnamurthy, C.M.Reaves, S.P.Denbaars, and P.M.Petroff, *Appl. Phys. Lett.* **63**, 3203 (1993)
- 4 J.M.Moison, F.Houzay, F.Barthe, L.Leprince, E.Andre, and O.Vatel, *Appl. Phys. Lett* **64**, 196 (1994)
- 5 N.N.Ledentsov *et al Proc. of the 22nd ICPS Vancouver*, 1994, D.J. Lockwood, ed. (World Scientific, Singapore, 1995), vol. 3, p. 1855, M.Grundmann *et al, Phys.Stat.Sol.(b)*, **188**, 249 (1995) S.S.Ruvimov *et al, Phys.Rev. B* **51**, 14766 (1995); G.E.Cirlin *et al, Appl.Phys.Lett.*, **67**, 97 (1995)
- 6 V.A. Shchukin, N.N. Ledentsov, P.S. Kop'ev and D.Bimberg, *to be published*
- 7 N.Kirstaedter *et al, Electronics Letters* **30**, 1416 (1994)
- 8 N.N. Ledentsov *et al, to be published*
- 9 M. Grundmann *et al, to be published*
- 10 M.Grundmann *et al, Phys.Rev.Lett.***74**, 4043 (1995)
- 11 E.I.Rashba, *Sov. Phys. Semicond.* **8**, 807 (1994)
- 12 N.N. Ledentsov *et al, to be published*
- 13 Z.H. Ming, Y.L. Soo, S. Huang, Y.H. Kao, K. Stair, G. Devane, C. Choi-Feng, *Appl. Phys. Lett.* **66**, 165 (1995)

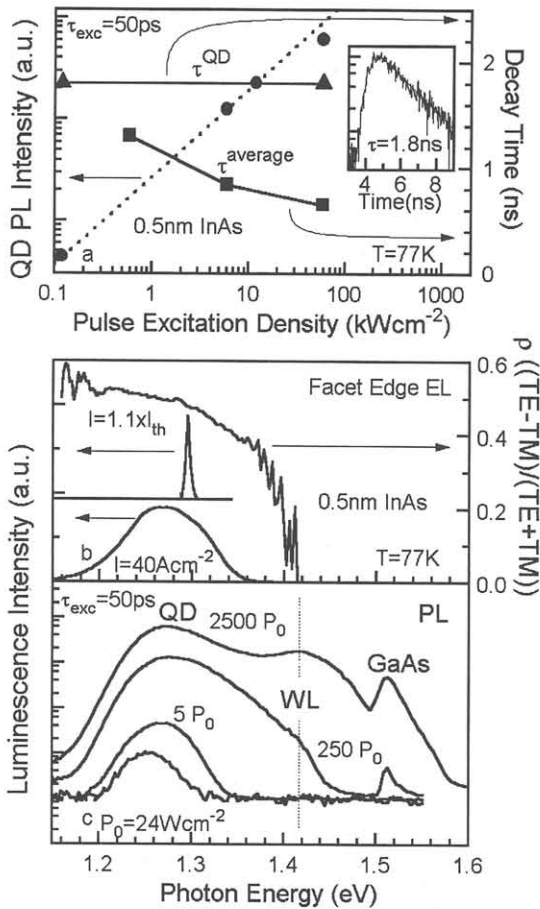


Fig. 1

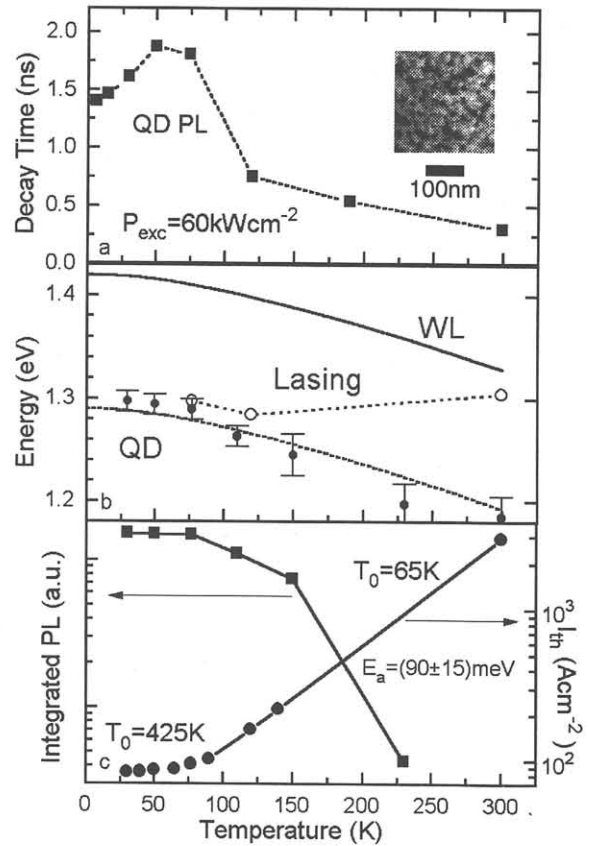


Fig. 2